TU Delft

Delft University of Technology

Document Version
Final published version

Licence
CC BY

Citation (APA)
Trikannad, S. A., van Halem, D., Foppen, J. W., & van der Hoek, J. P. (2023). The contribution of deeper layers in slow sand filters to pathogens removal. *Water Research*, *237*, Article 119994. https://doi.org/10.1016/j.watres.2023.119994

Important note
To cite this publication, please use the final published version (if applicable).
Please check the document version above.

Copyright
In case the licence states “Dutch Copyright Act (Article 25fa)”, this publication was made available Green Open Access via the TU Delft Institutional Repository pursuant to Dutch Copyright Act (Article 25fa, the Taverne amendment). This provision does not affect copyright ownership.
Unless copyright is transferred by contract or statute, it remains with the copyright holder.

Sharing and reuse
Other than for strictly personal use, it is not permitted to download, forward or distribute the text or part of it, without the consent of the author(s) and/or copyright holder(s), unless the work is under an open content license such as Creative Commons.

Takedown policy
Please contact us and provide details if you believe this document breaches copyrights.
We will remove access to the work immediately and investigate your claim.

This work is downloaded from Delft University of Technology.

Water Research 237 (2023) 119994

Contents lists available at ScienceDirect

Water Research

journal homepage: www.elsevier.com/locate/watres

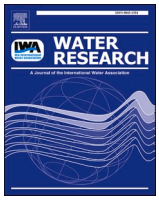

The contribution of deeper layers in slow sand filters to pathogens removal

Shreya Ajith Trikannad [a,*], Doris van Halem [a], Jan Willem Foppen [a], Jan Peter van der Hoek [a,b]

[a] Department of Water Management, Delft University of Technology, Building 23 Stevinweg 1, 2628, Delft, the Netherlands
[b] Waternet, Korte Ouderkerkerdijk 7, 1096 AC, Amsterdam, the Netherlands

ARTICLE INFO

Keywords:
Slow sand filters
Pathogen removal
Schmutzdecke
One-site kinetic model
Mature biofilm

ABSTRACT

Slow Sand Filtration is popular in drinking water treatment for the removal of a wide range of contaminants (e.g., particles, organic matter, and microorganisms). The *Schmutzdecke* in slow sand filters (SSFs) is known to be essential for pathogen removal, however, this layer is also responsible for increased head loss. Since the role of deeper layers in bacteria and virus removal is poorly understood, this research investigated the removal of *E.coli* WR1 and PhiX 174 at different depths of a full-scale SSF. Filter material from top (0–5 cm), middle (5–20 cm) and deep (20–35 cm) layers of an established filter was used in an innovative experimental set-up to differentiate physical-chemical and biological removal processes. In the analysis, we distinguished between removal by biological activity, biofilm and just sand. In addition, we modelled processes by a one-side kinetic model. The different layers contributed substantially to overall log removal of *E.coli WR1* (1.4–1.7 $\log_{10}$) and PhiX 174 (0.4–0.6 $\log_{10}$). For *E.coli WR1*, biological activity caused major removal, followed by removal within biofilm and sand, whereas, removal of PhiX 174 mainly occurred within sand, followed by biofilm and biological activity. Narrow pore radii in the top layer obtained by micro-computed tomography scanner suggested enhanced retention of bacteria due to constrained transport. The retention rates of *E.coli WR1* and PhiX 174 in top layer were four and five times higher than deeper layers, respectively (k_{ret} 1.09 min^{-1} vs 0.26 min^{-1} for *E.coli WR1* and k_{ret} 0.32 min^{-1} vs of 0.06 min^{-1} for PhiX 174). While this higher rate was restricted to the *Schmutzdecke* alone (top 5 cm), the deeper layers extend to around 1 m in full-scale filters. Therefore, the contribution of deeper layers of established SSFs to the overall log removal of bacteria and viruses is much more substantial than the *Schmutzdecke*.

1. Introduction

Slow sand filtration, one of the earliest water treatment processes, has been a major contributor to drinking water safety (Chan et al., 2018; Chen et al., 2021; Haig et al., 2011; Maurya et al., 2020). In the past decades, slow sand filters (SSFs) have demonstrated the capacity to effectively remove turbidity, dissolved organic matter and a wide range of pathogenic microorganisms (bacteria, viruses and protozoa). However, in recent times, the focus has also been on the removal of biodegradable organic matter to increase biological stability of drinking water (van der Kooij et al., 2017). In low-resource settings, intermittently operated SSF, popularly known as the "biosand filter" (BSF) has been a promising household-scale point-of-use (POU) technology for removal of microbes from drinking water. The BSF has been highly successful when measured by user-satisfaction, durability and simplicity of design and operation (Elliott et al., 2011; Napotnik et al., 2020). While SSFs differ from BSF in design and operation, they offer a major benefit of chemicals-free turbidity and pathogen removal, compared to any direct competing technologies like membrane filtration, coagulation, ozonation and few more (de Oliveira and Schneider, 2019). Drinking water treatment plants in the Netherlands, the United Kingdom, Sweden, Brazil and many more use SSFs as a third or final treatment step in drinking water production due to their low energy consumption and high efficiency. When drinking water is distributed without residual disinfectants such as chlorine (Sousi et al., 2020), utilities opt for a multi-stage treatment scheme where SSFs are the final treatment step to produce microbiologically safe and biologically stable drinking water (van der Kooij et al., 2017).

While SSFs are known to be safe and robust, there is also consensus that there are a few drawbacks and limitations in operation. The filters have a large land footprint as they are designed to operate at low filtration rates. The *Schmutzdecke*, a dense biofilm in the top layer of

Abbreviations: SSF, Slow sand filter; *E.coli*, *Escherichia coli*; BSF, Biosand filter; HNA, High nucleic acid; LRV, Log reduction value.

* Corresponding author.
E-mail address: s.a.trikannad@tudelft.nl (S.A. Trikannad).

https://doi.org/10.1016/j.watres.2023.119994
Received 14 February 2023; Received in revised form 20 April 2023; Accepted 21 April 2023
Available online 24 April 2023
0043-1354/© 2023 The Author(s). Published by Elsevier Ltd. This is an open access article under the CC BY license (http://creativecommons.org/licenses/by/4.0/).

SSFs is considered a key barrier for pathogens and other contaminants but overgrowth of biomass in this layer increases head loss in the filter (Andreoli and Sabogal-Paz, 2020; Dizer et al., 2004; Hijnen et al., 2007; Schijven et al., 2013). As a result, cleaning techniques like scraping and wet harrowing are applied which in turn demand a long ripening period of 6–8 weeks to re-establish the *Schmutzdecke* and restore filter performance (Huisman and Wood, 1974; Jenkins et al., 2011).

The importance of *Schmutzdecke* in SSFs is promoted by high microbial abundance, diversity, and a broad range of functions compared to deeper layers of the sand bed (Chen et al., 2021). Stratification of biomass with depth is not surprising as substrate concentration and biomass acting on substrates are highest at the surface of the sand bed. Thus, purification capacity and associated processes may be stratified over the filter height (Chen et al., 2021; Lee et al., 2014; Tatari et al., 2016). Recent investigation on mature full-scale SSFs showed that removal of the *Schmutzdecke* did not impact coliform counts and flow cytometry bacterial profiles in terms of intact cells and high nucleic acid content (HNA) in effluent water (Chan et al., 2018). They reported that deeper layers in mature filters operating for several years may have extensive biofilms with microbial community required for producing consistent microbial water quality. Generally, during scraping, the *Schmutzdecke* and the top few centimetres (2–5 cm) of sand are removed but deeper layers are retained unaltered. Pfannes et al. (2015) observed 16S rRNA gene copy numbers of around 10^6 copies/mL in the deep sand bed. Although the count is less than 10^{11} copies/mL commonly found in the *Schmutzdecke*, the total volume occupied by the sand bed is much greater than the volume in the *Schmutzdecke*. Oh et al. (2018) observed that microorganisms in the deeper layers grew faster by metabolizing more easily degradable organic matter compared to microbes in the *Schmutzdecke*.

Biofilms in both *Schmutzdecke* and sand bed can entrap cells and support microbial interactions, thus, SSF performance may be a balance between processes in different layers of sand bed (Chan et al., 2018; Pfannes et al., 2015). For example, bacteria and protozoa removal occurred mainly in the *Schmutzdecke* but virus removal improved with filter depth (Elliott et al., 2008). While the influence of *Schmutzdecke* on pathogen removal and associated mechanisms has been studied extensively (Hijnen et al., 2004; Schijven et al., 2013; Unger and Collins, 2008), the contribution of deeper depths in removal has not received much attention in the past. Previous studies evaluating filter performance have been largely performed on filters at lab or pilot scale where a sand bed microbial community has not had years to establish (Haig et al., 2014; Hijnen et al., 2004; Pfannes et al., 2015; Unger and Collins, 2008). In filters without an established microbial community in the deeper layers, changes in treated water quality could be more coupled to the status of the *Schmutzdecke* (Chan et al., 2018). Therefore, understanding of removal processes in both *Schmutzdecke* and deep sand bed in established full-scale filters is crucial to enable improvements in design and operational procedures of SSFs, in terms of new filter designs (bed height) and cleaning procedures for biomass preservation within the filter.

In this study, we explored bacteria and virus removal capacity of *Schmutzdecke* and deeper layers of an established SSF to distinct various co-occurring removal processes (including, straining, attachment and microbial inactivation). The top and deeper depths of the filter may be evaluated as separate systems due to vast differences in the physical and biological characteristics of sand that influence microbial transport. Hence, knowledge of stratification of biotic and abiotic-induced processes that aid microbial removal is important for further optimization and promotion of the SSF technology. In this study, we hypothesized that deeper layers contribute substantially to *E.coli WR1* and PhiX 174 bacteriophage removal due to a mature biofilm in the sand bed. Therefore in an innovative experimental set-up, the removal capacity and transport of indicator enteric pathogens *E.coli WR1* and PhiX 174 were investigated at different depths of a full-scale filter. To investigate the contribution of physical, chemical and biological processes in removal, sand from different depths was investigated directly, after inactivation of microbial activity by sodium azide and after incineration to remove the biofilm. The retention and reentrainment behaviour of *E. coli WR1* and PhiX 174 at different depths were modelled using a one-site kinetic model. A micro-computed tomography scanner (Micro-CT) and environmental scanning electron microscopy (ESEM) were employed to investigate the influence of porosity and sand characteristics on microbial transport at different depths.

2. Materials and methods

2.1. Sampling at full-scale slow sand filter

An established SSF producing drinking water for over 67 years (built in 1955) at a drinking water treatment plant of Dunea (located at Katwijk), a drinking water utility in the Netherlands was used in this study. The plant receives raw water from the river Meuse and is further treated by managed aquifer recharge in the dunes, pellet softening, aeration, rapid sand filtration with powdered activated carbon dosing and lastly slow sand filtration. The SSF in our study has been in operation for approx. 28 years without sand replacement. At the moment of sand sampling, the filter had a sand bed height of 0.9 m with grain size of 0.4–0.6 mm, followed by 0.3 m of gravel layer (4–6 mm) and 0.12 m of underdrains for uniform passage of filtered water. The hydraulic loading was 0.4 m/h. The in-situ water temperature at the treatment plant was mostly stable, between 10 and 12 °C, as seasonal fluctuation was regulated during dune filtration. Over a period of operation, generally a few years, the filters become clogged with biomass. To restore water flow, the top layers (2–5 cm) of the SSF including *Schmutzdecke* is removed by mechanical scraping. The filter in this study was last scraped 653 days ago.

During one such scraping event, intact sand samples from mature SSF was sampled up to a depth of 40 cm. Sand was core-sampled from depths 0–5 cm (top), 5–20 cm (middle) and 20–35 cm (deep) by inserting and gently removing a sterile plexiglass cylinder. The cylinder had an inner diameter of 2.5 cm and height of 5 cm for top layer and 15 cm for middle and deep layers, and closed at the top with a rubber stopper. Sampling with the cylindrical cores provided the advantage to take undisturbed in-situ sand samples without impacting the 3D structure and was further transformed into columns for the experiments. Two sand cores from each depth were sampled at two randomly selected locations to be used for duplicate column experiments.

2.2. Experimental set-up

The experimental set-up consisted of small plexiglass columns with inner diameter of 2.5 cm and bed height of 5 cm for sand from top layer (0–5 cm) and 15 cm for sand from middle (5–20 cm) and deep layer (20–35 cm). The core-sampled sand from each depth was operated in columns under three conditions to simulate scenarios of physical, chemical and biological processes in treatment: active biofilm, inactive biofilm and no biofilm. The sand was prepared as per the following:

i) Active biofilm sand: Sand directly obtained from the full-scale SSF (as described in Section 2.1). The three depths in consideration had different active biomass concentrations, with the highest bioactivity in the top layer and the lowest in the deep layer as shown by ATP analyses in Figure S1.
ii) Inactive biofilm sand: Microbial activity on sand from three depths and in the water phase was suppressed by continuously dosing sodium azide at a concentration of 6-mM (390 mg/L) (Elliott et al., 2011). Dosing was continued for three days until no biological activity was detected. The activity was determined by measuring cellular ATP on 1 g of sand using the Deposit & Surface Analysis kit (DSA) (LuminUltra Technologies Ltd.) according to the manufacturer's protocol.

iii) No biofilm sand: Biofilm on sand from three depths was destroyed by drying sand at 105 °C and then ignited at 440 °C in a muffle furnace as per British Standard (British Standards Institution, 1990b; Rodgers et al., 2004). The biofilm was burnt off at this temperature, leaving behind a mixture of sand and ash. The sand mixture from 3 depths was washed through a 53-μm sieve and filled into their respective columns.

The influent feeding the full-scale SSFs at the water treatment plant was used as influent for the columns at a filtration rate of 0.4 $m^3/m^2/h$ to replicate full-scale SSF condition. The pore volume and porosity in the columns were determined using deuterium (^2H) as a tracer according to Bertelkamp et al. (2016). Further, the columns were challenged with enteric bacteria and virus indicators *E.coli* WR1 and PhiX 174 bacteriophages.

2.3. E.coli WR1 and PhiX 174 preparation and enumeration

The experiments were carried out with *E.coli* WR1 (NCTC 13,167) and bacteriophage PhiX 174 (ATCC 13,706-B1). *E. coli* WR1 is widely used as an indicator of enteric bacteria in drinking water studies (Eisfeld et al., 2022; Schijven et al., 2013) and is used here as a reference for bacterial removal. A highly concentrated suspension of *E. coli* WR1 was prepared by growing in buffered peptone water for 18 h at 37 °C, harvested by centrifugation at 3000 g for 5 min and washing in sterile water as per ISO 9308–1. *E.coli WR1* was enumerated by membrane filtration and incubation onto Chromocult agar for 24 h at 37 °C. PhiX 174 is an icosahedral, single-stranded DNA-phage with a diameter of 26 nm and an isoelectric point of 4.4 (Chrysikopoulos and Aravantinou, 2012; Soliman et al., 2020a, 2020b). PhiX 174 is generally seen as a good viral surrogate due to its size and shape resemblance to several human enteroviruses such as poliovirus, norovirus, etc. as well as its low hydrophobicity and stability (Bicudo et al., 2021; Oudega et al., 2021). Although PhiX174 may not be an ideal conservative colloidal tracer, somatic coliphages have gained special importance in Europe in recent years as a reliable viral faecal indicator due to their high prevalence in sewage and persistence in the environment (Oudega et al., 2021). A highly concentrated suspension of PhiX 174 (10^{11} pfu/ml) was prepared and concentrations were assayed as described in ISO-10,705.

2.4. Spiking of E.coli WR1 and PhiX 174

Challenge water was prepared by dosing *E. coli* WR1 or PhiX 174 stock solution to the influent at a concentration of 10^5 to 10^6 cfu/ml and stirred (150 RPM) to prevent settling. The influent concentration was sampled in triplicate: two times before spiked water was distributed and one time after the spiking was done. Challenge experiments with active biofilm, inactive biofilm and no biofilm sand were performed on days 5, 10 and 13, respectively. Spiking was done by lowering the supernatant slightly above the sand bed and dosing the challenge water using a peristaltic pump. After spiking for 2–3 pore volumes (PVs), influent water free of *E.coli* WR1 or PhiX 174 was dosed for the next 8 PVs. Effluent samples were collected in 250 ml sterile bottles every 5 min for the first 4–5 PVs and every 10 min for the next 5 PVs. The collected samples were refrigerated and further analysed on the same day to yield breakthrough curves.

2.5. Micro-computed tomography

The top layer column in active, inactive and no biofilm conditions were subjected to Micro-Computed Tomography (Micro-CT) (Phoenix Nanotom, Boston, MA, USA, 180 kV, 0.5 mA, with a maximum resolution 0.5–1.0 μm). Before imaging, sand columns were disconnected from influent and effluent lines while maintaining the sand bed saturated. ImageJ (http://rsb.info.nih.gov) was used to obtain porosity distribution and calculate pore radius.

2.6. Modelling transport of E.coli WR1 and PhiX 174

Transport of microorganisms in porous media is described by the advection-dispersion equation with first-order retention and reentrainment (Kianfar et al., 2022; Schijven et al., 2013):

$$\frac{\partial C}{\partial t} + \frac{\rho_b}{\theta}\frac{\partial S}{\partial t} = \lambda_L \nu \frac{\partial^2 C}{\partial x^2} - \nu \frac{\partial C}{\partial x} \quad (1)$$

$$\rho_b \frac{\partial S}{\partial t} = k_{ret}\,\theta C - \rho_b k_{reent} S \quad (2)$$

where C is the concentration of free microorganisms [cfu/ml or pfu/ml], S is the concentration of attached microorganisms [cfu/g or pfu/g], ρb is the dry bulk density [kg/m^3], θ is volumetric water content [m^3/m^3], t is time [min], λ_L is the dispersivity (cm^{-1}), ν is the pore water velocity [$cm.min^{-1}$], x is the travelled distance (cm), and k_{ret} and k_{reent} are retention and reentrainment rate coefficients, respectively [min^{-1}]. In this work, retention processes such as unfavourable and favourable attachment, hydrophobic interactions and straining are undertaken together under a single retention rate coefficient. While, reentrainment rate included detachment from previously (un)favourably attached microorganisms, or detachment of previously hydrophobically retained microorganisms.

2.7. Estimating contribution of physical, chemical and biological processes to removal

The estimation of contribution of removal of *E.coli* WR1 and PhiX 174 by intact biofilm (assumed as predation, grazing and enzyme-induced inactivation), biofilm (assumed as straining, hydrodynamic interaction and favourable attachment) and sand only (assumed as favourable and unfavourable attachment) was performed using Log Reduction Values (LRVs) in "active", "inactive" and "no biofilm" experiments as inputs. Intact biofilm induced removal was determined by subtracting LRVs in "inactive biofilm" from LRVs in "active biofilm" experiments. The contribution of removal by sand alone was directly obtained from LRVs in "no biofilm" experiment. Further, biofilm led removal was calculated from the difference of LRVs in "inactive" and "no biofilm" experiments. In the "no biofilm" experiments, the effects of biofilm removal and sand repacking (see Section 2.2), which clearly affected filter bed pore structure were neglected.

2.8. Data analysis

Data represents the mean and standard error (SE) of duplicate microbial assays in duplicate columns ($n = 4$). Statistical comparison of means of *E.coli* WR1 and PhiX 174 removal at depths was performed by ANOVA (factor: depth). Pairwise comparison of statistically different means in a series was performed with a pos-hoc Tukey test ($p = 0.05$). Means for different filter media conditions for each depth were also compared using ANOVA (factor: condition) and further with pos-hoc Tukey test.

3. Results

3.1. E.coli WR1 and PhiX 174 attenuation in active biofilm sand

Fig. 1 shows breakthrough curves (BTCs) of *E.coli* WR1 and PhiX 174 (both data and fitted curves) in top, middle and deep layer columns under active biofilm conditions. All BTCs are characterized by a climbing limb, a plateau phase, a declining limb, and finally a gradual declining tail. The BTCs of *E.coli* WR1 exhibit a very low relative breakthrough concentration in the range of 0.02–0.03 in top, middle and deep layers, resulting in LRVs of 1.69, 1.52 and 1.41 log_{10}, respectively (Fig. 1, Table 1). It is important to note that sand bed height was 5 cm in the top layer column and 15 cm in middle and deep layer columns. As a

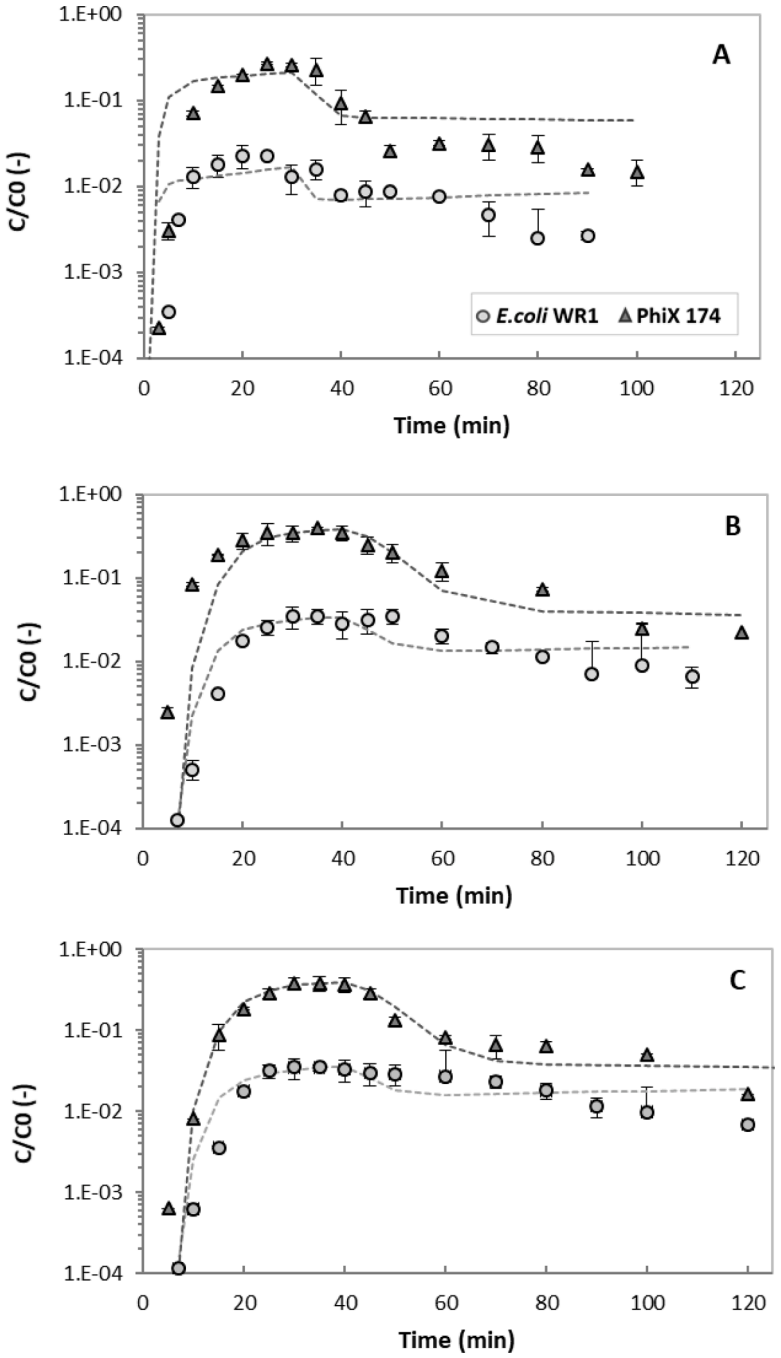

Fig. 1. Breakthrough curves of *E.coli* WR1 and PhiX 174 in top (A), middle (B) and deep (C) layer columns under active biofilm condition. Data represents the mean and standard error (SE.) of duplicate microbial assays in duplicate columns ($n = 4$). Dotted lines are fitted models obtained from Hydrus-1D and the symbols are corresponding experimental data (in the same colour as the dotted lines).

result, the estimation of log removal per cm showed removal of 0.33 $\log_{10}$/cm in the top layer, substantially higher compared to 0.10–0.12 $\log_{10}$/cm in the middle and deep layer columns. ANOVA tests conducted for removal using depths as the independent variable produced p-values below 0.05 ($F = 11.09$, $p = 0.0001$, $df = 2$) showing that LRVs at three depths were statistically different. The R^2 values between 0.83–0.95, indicated that breakthrough could be well described by one retention rate and one reentrainment rate parameter. *E.coli* WR1 displayed a k_{ret} of 1.09 min^{-1} in the top layer, which was 5 times higher than k_{ret} of 0.26 min^{-1} in the middle and deep layers.

The BTCs of PhiX 174 showed a high relative breakthrough concentration in the range of 0.27–0.39, which was 10 times higher than *E. coli* WR1 relative breakthrough concentration. The BTCs resulted in poor but comparable LRVs of 0.56, 0.41 and 0.42 $\log_{10}$ in top, middle and deep layers, respectively ($F = 1.91$, $p = 0.142$, $df = 2$). Further, the estimation of log removal per cm showed removal of 0.12 $\log_{10}$/cm in top layer, 4 times higher than removal of 0.03 $\log_{10}$/cm in middle and deep layers. ANOVA tests performed using depth as an independent variable produced p-values above 0.05 ($F = 2.23$, $p = 0.181$, $df = 2$), meaning that for PhiX 174 the influence of depths in removal is statistically insignificant. The BTCs were well described by one retention rate parameter and one re-entrainment rate parameter shown by R^2 values greater than 0.9. Similar to the observations for *E.coli* WR1, PhiX 174 showed higher k_{ret} of 0.32 min^{-1}, compared to k_{ret} of 0.06 min^{-1} in

Table 1
Model parameters for *E.coli* WR1 and PhiX 174 BTCs in top, middle and deep layer columns under active biofilm condition.

Condition	Model organism	Depths	Hydrus-1D results					Calculated results		
			k_{ret} (min^{-1})		k_{reent} (min^{-1})		R^2	C/C_0 peak	$-\log_{10}(C/C_0)/x$	$-\log_{10}(C/C_0)$
			EST.	SE.	EST.	SE.				
Active biofilm	*E.coli* WR1	Top	1.09	0.07	0.01	0.002	0.83	0.02	0.33	1.69
		Middle	0.26	0.01	0.01	0.001	0.93	0.03	0.12	1.52
		Deep	0.26	0.01	0.01	0.001	0.93	0.04	0.10	1.41
	PhiX 174	Top	0.32	0.04	0.01	0.004	0.95	0.27	0.12	0.56
		Middle	0.06	0.004	0.004	0.003	0.90	0.39	0.03	0.41
		Deep	0.06	0	0.004	0.002	0.94	0.38	0.03	0.42

Data represents the mean and standard error (SE.) of duplicate microbial assays in duplicate columns ($n = 4$). R^2= coefficient of determination to evaluate model fit to the data; $-\log_{10}(C/C_0)$= overall log removal per column; x= distance in cm; $-\log_{10}(C/C_0)/x$= log removal per cm; EST.= estimated value.

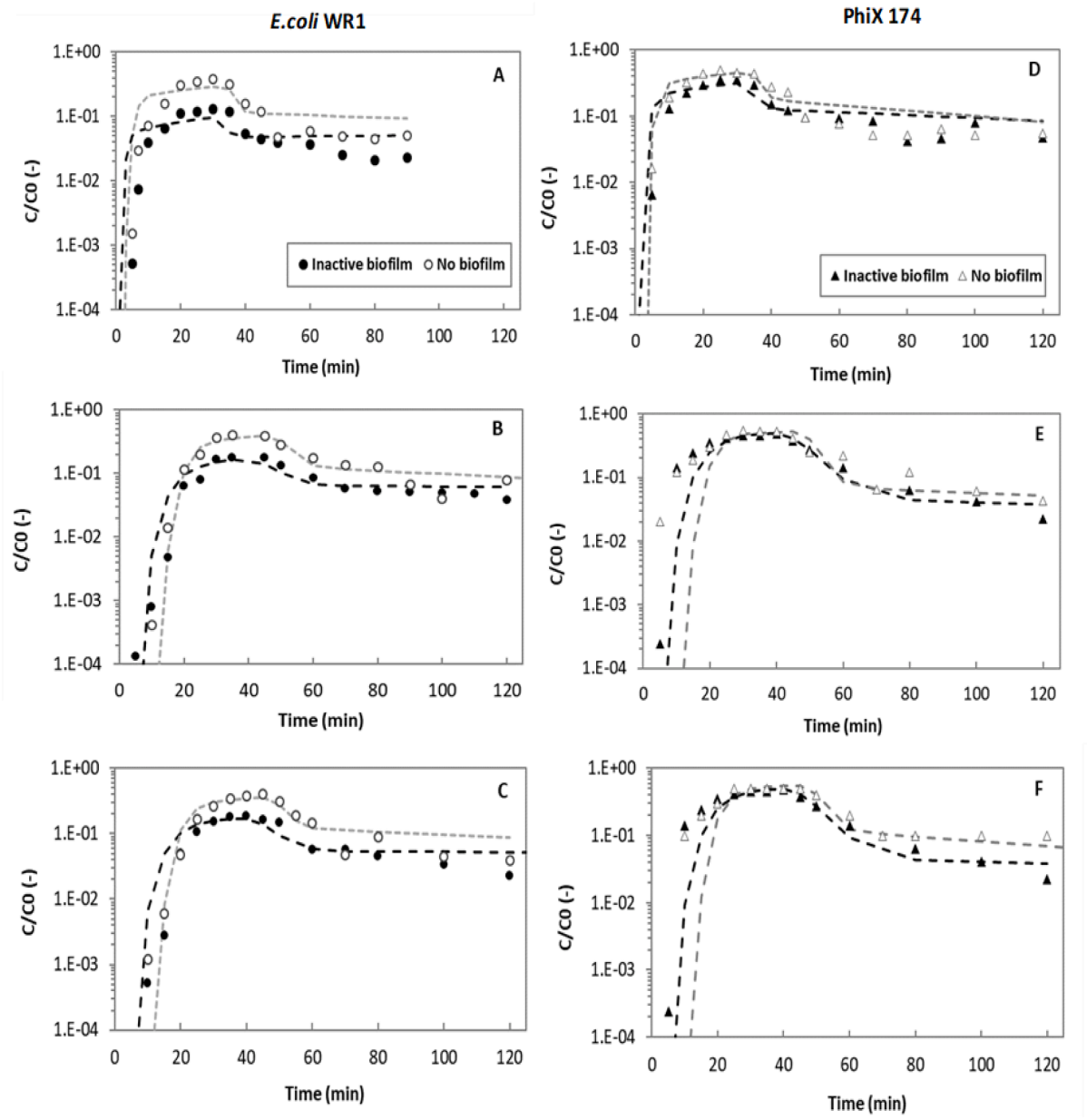

Fig. 2. Breakthrough curves of *E.coli* WR1 and PhiX 174 in top (A,D), middle (B,E) and deep (C,F) layer columns in inactive biofilm and no biofilm conditions. Data represents the mean and standard error (SE.) of duplicate microbial assays in duplicate columns ($n = 4$). Dotted lines are fitted models obtained from Hydrus-1D and the symbols are corresponding experimental data (in the same colour as the dotted lines).

middle and deep layers.

3.2. E.coli WR1 and PhiX 174 attenuation in inactive biofilm and no biofilm sand

Upon suppression of microbial activity by sodium azide, LRVs of *E. coli* WR1 in the top, middle and deep layers drastically decreased by 0.80, 0.80 and 0.70 $\log_{10}$ to LRVs of 0.92, 0.71 and 0.69 $\log_{10}$, respectively. It is evident from the BTCs in Fig. 2 that the relative breakthrough concentrations and tails in inactive biofilm conditions were at least one order of magnitude higher than the BTCs under active biofilm conditions. Statistical testing showed that *E.coli* WR1 reductions were significantly lower (by 0.7–0.8 $\log_{10}$) after microbial activity suppression ($F = 15.36$, $p = 0.0004$, $df = 1$). Lower removal in inactive biofilm experiments is also reflected by the low retention rates in all three depths.

In the no biofilm experiments, LRVs of *E.coli* WR1 significantly reduced by 0.50, 0.30 and 0.30 $\log_{10}$ to 0.42, 0.42 and 0.44 $\log_{10}$ in top, middle and deep layers, respectively ($F = 16.94$, $p = 0.0003$, $df = 2$). This was also depicted by a further reduction in k_{ret} as shown in Table 2.

While PhiX 174 displayed a similar behaviour as *E.coli* WR1, the removal was low. The absence of microbial activity caused LRVs to reduce by 0.20, 0.20 and 0.15 $\log_{10}$ to 0.46, 0.35 and 0.34 $\log_{10}$ in top, middle and deep layers, respectively also displayed by lower k_{ret} (Table 2). Although the variations seem minimal, ANOVA test revealed a statistically significant removal before and after bioactivity inhibition ($F = 21.56$, $p = 0.011$, $df = 1$). No biofilm experiments further reduced LRVs by 0.20, 0.10, 0 $\log_{10}$ to 0.31, 0.26 and 0.28 $\log_{10}$ in top, middle and deep layers, respectively. The influence of loss of biofilm was statistically significant in top and middle layers ($F = 11.16$, $p = 0.0004$, $df = 1$) but not in the deep layer ($F = 1.13$, $p = 0.05$, $df = 1$) (Table 2).

3.3. Micro-computed tomography scanner

The biofilm dense *Schmutzdecke* may influence porosity in the top layer and alter flow path. Micro-computed tomography scanner (Micro-CT) was used to directly characterize the pore structure and porosity distribution in the top layer column in active, inactive and no biofilm conditions. A comparison of porosity profiles (Fig. 3A) shows that porosity in active and inactive biofilm columns is much lower than porosity in absence of biofilm. In the active biofilm column, porosity increased along the filter height; the lowest porosity of 0.27 was recorded near the column inlet which increased to 0.32 almost at the bottom of the sand bed (5 cm). The inactive biofilm column depicted the same trend in porosity distribution. On the other hand, the column without biofilm showed a consistent porosity in the range of 0.38–0.40 throughout the height of the sand bed. Further investigation on pore radius showed that pore radii in the column with no biofilm spanned between 15 and 75 μm, with a median around 35 μm (Fig. 3C). In the active and inactive biofilm columns, pore radii ranged between 1 and 35 μm, with a median of 15 μm (Fig. 3C). In active and inactive biofilm columns, pore radii of 1 μm, which are in the range of average size of *E. coli* WR1 made up 0.03–0.07% of the total pore volume.

4. Discussion

4.1. Significance of mature biofilm

This study showed that top, middle and deep layers of mature SSF caused substantial removal of *E.coli* WR1 (1.4–1.7 $\log_{10}$) and PhiX 174 (0.4–0.6 $\log_{10}$) indicating the significance of mature biofilm in the sand bed. *Schmutzdecke* is described as a visibly thick, brownish slimy layer, unlike the biofilms in deeper layers that can only be visualized under the microscope. Hence, a general assumption is that pathogen removal by microbial activity associated processes like predation, grazing or enzyme induced inactivation occurs mainly in the *Schmutzdecke* where biological activity is the highest (Chen et al., 2021; Schjiven et al., 2013). Complementary to the previous observations, we found that microbial activity in intact biofilm contributed to 0.70–0.80 $\log_{10}$ of *E. coli* WR1 removal at all three depths (Table 3). Meanwhile, the intact biofilm slightly influenced PhiX 174 removal with 0.10 $\log_{10}$ at all three depths. In biological filters, stratification of biomass and bioactivity is observed due to environmental and chemical gradients (e.g., DOC, NH_4^+) (Chen et al., 2021). Despite these variations, the substantial contribution of deeper depths to overall bacteria and virus log removal suggests the importance of a well-functioning biofilm in the sand bed.

Mature biofilms in filters functioning over a while have been reported to own different physical and biological properties such as thickness, morphology and microbial community composition compared to young biofilms in newly established filters (Boe-Hansen et al., 2002; Bai et al., 2022; Haig et al., 2015). In this study, we observed that biofilm associated removal by straining, hydrodynamic interaction, and favourable attachment contributed to *E.coli* WR1 removal of 0.5 $\log_{10}$ in the top layer and 0.3 $\log_{10}$ in middle and deep layers (Table 3). The contribution to PhiX 174 removal was rather low, between 0.1–0.2 $\log_{10}$. Earlier studies showed *Schmutzdecke* thickness as one of the major factors increasing pathogen removal in SSFs (Schijven et al., 2013). Increased biofilm thickness by biomass accumulation is a consequence of filter ageing or maturation (Elliot et al., 2011; Hijnen et al., 2007; Schijven et al., 2013). Enhanced attachment and straining of bacteria

Table 2
Model parameters for *E.coli* WR1 and PhiX 174 BTCs in top, middle and deep layer columns in inactive biofilm and no biofilm conditions.

Condition	Model organism	Depths	Hydrus-1D results					Calculated results		
			k_{ret} (min^{-1})		k_{reent} (min^{-1})		R^2	C/C_0 peak	$-\log_{10}(C/C_0)/x$	$-\log_{10}(C/C_0)$
			EST.	SE.	EST.	SE.				
Inactive biofilm	*E.coli* WR1	Top	0.57	0.06	0.01	0.004	0.95	0.12	0.18	0.92
		Middle	0.10	0.01	0.01	0.002	0.97	0.19	0.05	0.72
		Deep	0.10	0.01	0.01	0.002	0.98	0.2	0.05	0.70
	PhiX 174	Top	0.27	0.03	0.02	0.004	0.96	0.35	0.09	0.46
		Middle	0.03	0.004	0.01	0.004	0.91	0.45	0.02	0.35
		Deep	0.04	0.003	0.01	0.003	0.93	0.46	0.02	0.34
No biofilm	*E.coli* WR1									
		Top	0.23	0.03	0.01	0.004	0.94	0.38	0.08	0.42
		Middle	0.05	0.003	0.01	0.002	0.95	0.38	0.03	0.42
		Deep	0.06	0.004	0.01	0.002	0.98	0.37	0.03	0.43
	PhiX 174	Top	0.17	0.02	0.01	0.004	0.98	0.49	0.06	0.31
		Middle	0.03	0.01	0.01	0.01	0.83	0.55	0.02	0.26
		Deep	0.03	0.004	0.01	0.01	0.90	0.53	0.02	0.28

Data represents the mean and standard error (SE.) of duplicate microbial assays in duplicate columns ($n = 4$). R^2= coefficient of determination to evaluate model fit to the data; $-\log_{10}(C/C_0)$= overall log removal per column; x= distance in cm; $-\log_{10}(C/C_0)/x$= log removal per cm; EST.= estimated value.

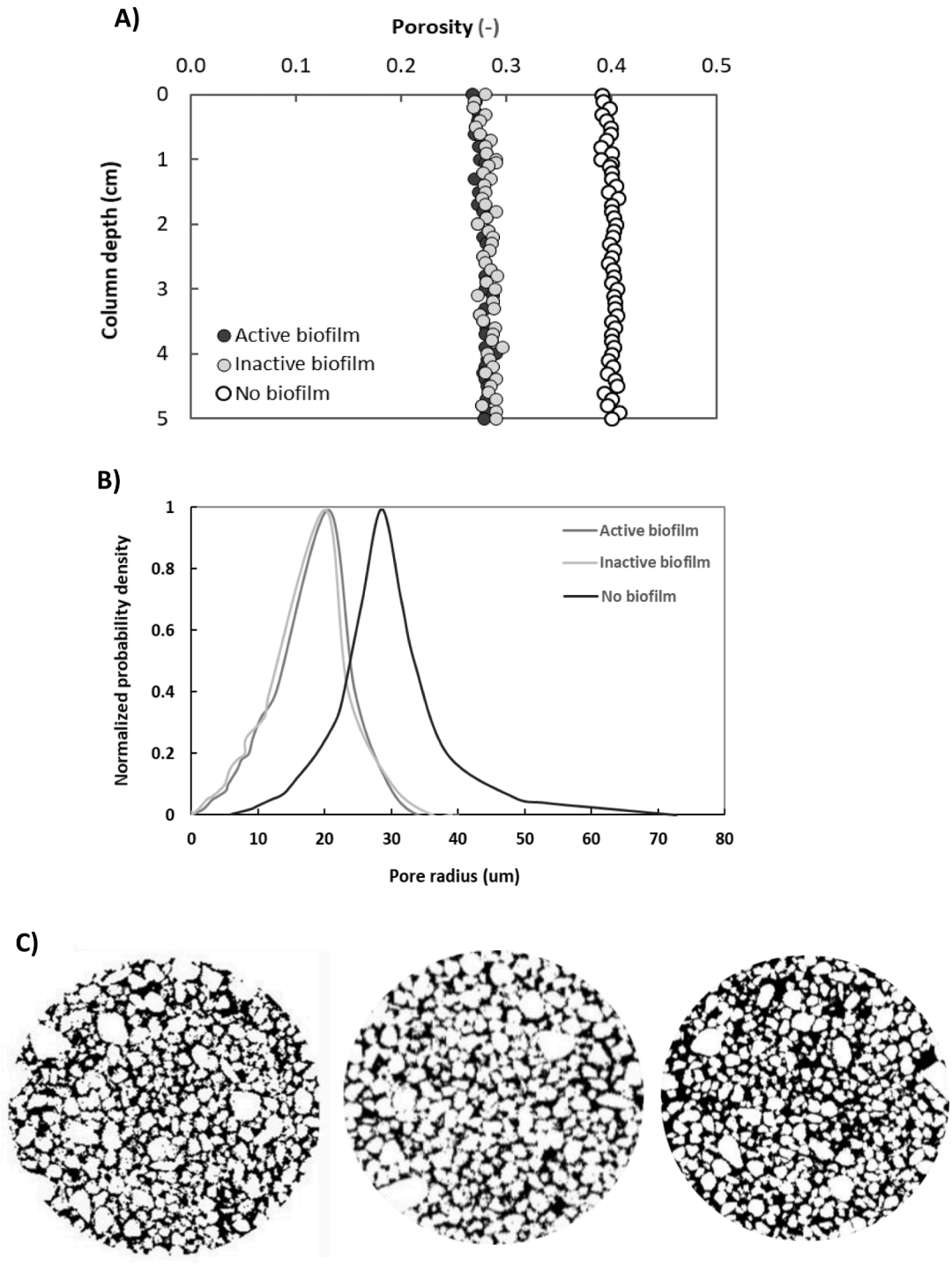

Fig. 3. Top layer column analysed using Micro-computed tomography scanner under active, inactive and no biofilm conditions. A) Porosity distribution along the column bed height, B) normalized probability density of pore radius, C) Micro-CT slices from 1 cm depth in the top layer showing intensity response of sand grains (white) and flow channels or pores (black).

and viruses have been observed for biofilms with higher thickness compared to relatively thin biofilms (Afrooz and Boehm, 2016). The favourable retention of bacteria and viruses in biofilm coated surface vs no biofilm surface is shown by higher retention rates in the former, thus depicting different transport behaviour (Fig. 1 and 2).

Biological properties of biofilm such as microbial community abundance, diversity and evenness increase with filter maturation (Haig et al., 2015). In newly built SSFs where biofilm has not had years to develop, *Schmutzdecke* microbial community may be distinctive from that of the sand bed. In such young filters, treatment performance may be more coupled to the status of the *Schmutzdecke* (Chan et al., 2018). In mature SSFs, this will not be the case as consequent temporal changes are marginal (Haig et al., 2015). E.g., the overall community composition in the first 50 cm of the sand bed is similar for bacteria, archaea, and eukaryotes (Li et al., 2017; Wakelin et al., 2011; Haig et al., 2015). Even at low abundance, eukaryotic communities are strongly related to the removal of pathogenic bacteria by grazing and predation (Weber-Shirk and Dick, 1997a, 1997b; Stott et al., 2001; Haig et al., 2015). Based on these observations, biological removal processes may be prominent even in the deeper layers and not restricted to the *Schmutzdecke* as previously

Table 3
Contribution of intact biofilm, biofilm and sand to overall removal of *E.coli* WR1 and PhiX 174 at different depths.

Model organism	Filter depths	Microbial log removal			
		Per depth	Intact biofilm	Biofilm	Sand only
E.coli WR1	Top layer	1.69 ± 0.317	0.77 ± 0.254	0.50 ± 0.317	0.42 ± 0.254
	Middle layer	1.52 ± 0.317	0.81 ± 0.317	0.29 ± 0.317	0.42 ± 0.317
	Deep layer	1.41 ± 0.254	0.72 ± 0.190	0.25± 0.254	0.44 ± 0.254
PhiX 174	Top layer	0.56 ± 0.317	0.1 ± 0.254	0.14 ± 0.190	0.32 ± 0.254
	Middle layer	0.41 ± 0.254	0.06 ± 0.254	0.09 ± 0.190	0.26 ± 0.254
	Deep layer	0.42 ± 0.317	0.08 ± 0.254	0.06 ± 0.190	0.28 ± 0.190

Data represents the mean values from duplicate column experiments ($n = 2$). 95%-confidence intervals are given between brackets.

assumed.

4.2. Retention processes at different depths

Active and inactive biofilm on sand increased retention of *E.coli* WR1 as seen by higher k_{ret} values compared to no biofilm experiments at all three depths. The top layer caused four times higher k_{ret} of *E.coli* WR1, compared to middle and deep layers (1.09 min-1 vs 0.26 min-1). Similarly, for PhiX 174, the influence of active and inactive biofilm was prominent in top layer, i.e., 5 times higher k_{ret} in top layer than deeper layers. It is worthy to note that *E.coli* WR1 retention was greater than PhiX 174 at all three depths, however, the change in k_{ret} between top and deeper layers was greater for the latter. This highlights the value of top layer, in terms of surface functionality and biological activity on sand in virus removal. These observations indicate varying contribution of different retention processes at different depths for each type of microorganism.

From the modelling results we infer, based on literature, that retention processes like straining, hydrophobic interactions, and favourable and unfavourable attachment are occurring (Afrooz et al., 2018; Fu et al., 2023). Straining is caused when microbes are trapped in pore throats that are too small to allow passage (Foppen et al., 2005). We observed that biofilms decreased the pore radii sizes in the top layer from 15–70 μm to 0.5–35 μm. With narrow pores, chances of *E.coli* WR1 retention by straining is higher due to higher chance of collision with biofilm and large size of bacteria (He et al., 2020; Foppen et al., 2007). Additionally, strained bacteria would not be reentrained unless biofilm sloughing happens which is not the case in our experiments as shown by 100 times lower k_{reent} of *E.coli* WR1 than k_{ret} in the top layer. However, for viruses, physical straining within the biofilm is unlikely due to their small size, supported by relatively lower k_{ret} in the top layer. The fact that *Schmutzdecke* removal (scraping) reduced bacteria LRVs and not viruses in earlier studies (Hijnen et al., al.,2007; Schijven et al., 2013) may support the argument that straining may be an important retention mechanism for bacteria in the top layer, although role of other (biological) retention mechanisms such as predation, grazing, enzyme induced inactivation and attachment to biofilm cannot be excluded. Enhanced retention of *E.coli* WR1 and PhiX 174 in biofilm sand may also be supported by Extracellular Polymeric Substances (EPS) in biofilms. EPS components- proteins and polysaccharides could bind and form hydrophobic interaction with bacterial surface functional groups such as teichoic acids and phospholipids (Fu et al., 2023; Xiao and Wiesner, 2013). In addition, positively charged amine groups in EPS promote electrostatic attraction with negatively charged bacteria and viruses allowing for favourable attachment (Guo et al., 2015).

In middle and deep layers, the biomass levels were much lower than in the top layer suggesting the presence of relatively thin biofilms. k_{ret} in both depths was slightly higher in the presence of biofilm indicating their influence on retention processes. Porosity distribution in middle and deep layers was not investigated in this study but the trend of increasing porosity with depth in top layer suggests that microbial retention by straining may not be critical in deeper depths. However, the contribution of hydrophobic interactions, and favourable and unfavourable attachment cannot be overlooked. This study did not quantify the exact contribution of different retention processes to *E.coli* WR1 and PhiX removal as such an effort was beyond the scope of the present study.

Interestingly, k_{ret} of *E.coli* WR1 and PhiX 174 in no biofilm experiments was not negligible. Under no biofilm condition, removal is determined by clean bed collisions and the classic colloid filtration mechanisms (interception, Brownian diffusion, and gravitational deposition) of which interception and Brownian diffusion are likely most important for bacteria and virus removal, respectively (Afrooz et al., 2018; Bradford et al., 2003). At neutral pH as in our experiments, colloids (*E.coli* WR1/PhiX 174) and sand grain surface are both negatively charged and therefore repulsive (Tripathi et al., 2011). However, when the distance between colloids and sand grain is small enough (less than a few nm), the attractive Van der Waals force may become dominant, thus causing attachment (Foppen et al., 2005). On the other hand, favourable attachment of negatively charged bacteria/viruses can occur on patches of positively charged surfaces on sand grains. Hence, the higher intensity of k_{ret} for both *E.coli* WR1 and PhiX 174 in top layer may be attributed to relatively high concentration of Fe and Mn (oxides) in top layer sand as shown in Fig. S3 (B). Despite these differences, similar removal of *E.coli WR1* and PhiX 174 at different bed heights in top, middle and deep layers is likely caused by small sticking efficiency variations within the bacterium and virus population. Despite the variation in sticking efficiencies as reported in literature, Hijnen et al. (2004) and Schijven et al. (2013) observed that removal data of *E.coli WR1 were* concomitant with removal of thermotolerant coliforms and naturally present *E.coli* bacteria in pilot and full-scale filter studies. In terms of viruses, Elliott et al. (2008) observed higher reduction of human enteric virus (echovirus 12) than bacteriophages (MS2 and PRD1) in BSF, suggesting that virus removal depends upon the specific viral agent.

4.3. Balanced contribution of Schmutzdecke and deeper layers to microbial removal

In this study, we hypothesised that deeper layers in established SSFs contribute to substantial removal of bacteria and viruses due to mature biofilm in the sand bed. The estimated LRVs showed that *E.coli* WR1 removal was 0.33 $\log_{10}$/cm in top layer and 0.10 $\log_{10}$/cm in middle and middle-deep layers. Similarly, PhiX 174 removal was 0.12 $\log_{10}$/cm and 0.03 $\log_{10}$/cm for top and middle-deep layers, respectively. Although log removal/cm in deeper layers is 3.3 and 4 times lower than in top layer for *E.coli* WR1 and PhiX 174, respectively, the total volume of the deep sand is many times greater than that occupied by the *Schmutzdecke*/top layer. The study of Pfannes et al. (2015) showed that effective removal of faecal indicators occurred due to the *Schmutzdecke* in 14 week-old SSFs, however, microbial communities in influent and effluent water were indistinguishable by t-RFLP analysis of bacterial 16S rRNA. In (immature) filters where a deep sand bed biofilm was unable to transform the influent water for any number of reasons (time, inoculation), the influence of *Schmutzdecke* on filter function might have been more obvious (Chan et al., 2018). In mature SSFs, functional microbial community was observed to be highly similar even when sampled from different depths (Haig et al., 2015). Thus, biofilms in both *Schmutzdecke* and deep sand bed is essential for shaping the produced water quality.

Based on the finding that deeper layers of SSFs are important for bacteria and virus removal, it is recommended that reducing the height of the filter bed by repetitive scraping is avoided where possible. By

doing so, the treatment capacity of the deep sand bed in mature SSFs can be utilized, particularly after *Schmutzdecke* scraping, preventing lengthy filter downtime. Also, traditional practice to switch the deeper layers to the top when renewing the filter bed might need reconsideration, as disturbing the deeper bed biofilm might have negative effects on filter perfomance. The filters in our study were operated at relatively high filtration rates of 0.4 m/h (typical filtration rates- 0.05–0.2 m/h) (Haig et al., 2015; Schijven et al., 2013) and grain size of 0.4–0.6 mm (typical grain sizes- 0.15–0.3 mm) (Schijven et al., 2013) which might have influenced the stratification of microbial processes. It is therefore encouraged to consider varying filtration rates and grain sizes (both lower and higher than the values in this study) as to further investigate the benefit on bacteria and virus removal.

This research also showed that bacteria and virus attenuation could be improved by microbial activity, also in the deeper layers. The microorganisms inhabiting the biofilm is driven by environmental and chemical gradients (e.g., DOC, NH_4^+) (Bai et al., 2022; Chen et al., 2021). Typically, SSFs in many parts of the world operate without extensive pre-treatment. Thus, greater loads of particulate matter, organics, nutrients and microorganisms are introduced for continued development of biological activity in the filter. As a result, the contribution of microbial mechanisms to removal could be greater, favouring pathogen removal. However, more efforts should be made to explore the influence of influent water quality and microbial community composition on pathogen removal in mature SSFs. Regardless, filter operational procedures, specifically cleaning practices that aim towards biomass preservation would benefit optimized performance. For instance, partial retention of *Schmutzdecke* in the filter, in-situ hydraulic rinsing may be considered as alternatives to the conventional scraping to shorten the ripening process.

5. Conclusions

This study examined the removal capacity of two important indicator enteric pathogens *E.coli* WR1 and PhiX 174 at different depths of an established full-scale SSF. Filter material collected from selected depths was studied in an innovative experimental setup to differentiate physical, chemical and biological removal processes. The main findings were:

- *Schmutzdecke* and deeper layers of established SSF showed substantial contribution to *E.coli* WR1 and PhiX 174 log removal.
- *E.coli* WR1 removal was caused by active biofilm led processes like predation, grazing, enzyme induced inactivation at all three depths indicating the importance of mature biofilms in the sand bed. Furthermore, removal by straining, hydrodynamic interaction, favourable and unfavourable attachment by (inactive) biofilm and sand contributed to overall removal.
- In contrast, active and inactive biofilm marginally influenced PhiX 174 removal, mainly in the top layer. However, PhiX 174 removal was found to be mostly influenced by Brownian diffusion as the engine of collisions with the sand surface.
- One-site kinetic retention model showed higher retention rates for *E. coli* WR1 and PhiX 174 in the top layer. Physical-chemical factors, such as pore radii and, Mn and Fe oxides and biological factors like dense biomass were identified as potential impactors for better retention of bacteria and viruses in the top layer.
- The knowledge of underestimated removal capacity of deeper sand bed is a valuable contribution to optimizing the design and operation of SSFs in drinking water utilities.

Credit authorship contribution statement

Shreya Ajith Trikannad: Conceptualization; Data curation; Investigation; Methodology; Analysis; Data visualization; Validation; Software; Writing- Original Draft Preparation. **Doris van Halem:** Supervision; Conceptualization and guidance on design; Data visualization; Writing- Reviewing and Editing. **Jan Willem Foppen:** Kinetic modelling; Writing- Reviewing and Editing. **Jan Peter van der Hoek:** Supervision; Conceptualization and guidance on design; Data visualization; Writing- Reviewing and Editing.

Declaration of competing interest

The authors declare that they have no known competing financial interests or personal relationships that could have appeared to influence the work reported in this paper.

Data availability

Data will be made available on request.

Acknowledgements

This study was performed within NWO-Dunea-Vitens partnership programme. The programme is funded by NWO, the national research council of the Netherlands (Project No. 17831). We would like to acknowledge the contribution of Feiyang Liu to a part of the experimental work. We would like to thank Brent Pieterse (Dunea) and Erik Kraaijeveld for supporting us with full-scale filter sampling and transporting influent samples to the lab. We appreciate the support of technicians Arjan Thijssen for E-SEM and Ellen Meijvogel-de Koning for X-ray micro-tomography imaging. We would like to acknowledge the staff from TU Delft Waterlab, especially Armand Middeldorp and Jasper Krijn for their support in the laboratory.

Supplementary materials

Supplementary material associated with this article can be found, in the online version, at doi:10.1016/j.watres.2023.119994.

References

Afrooz, A.R.M.N., Boehm, A.B., 2016. Escherichia coli removal in biochar-modified biofilters: effects of biofilm. PLoS ONE 11 (12), 1–17. https://doi.org/10.1371/journal.pone.0167489.

Afrooz, A.R.M.N., Pitol, A.K., Kitt, D., Boehm, A.B., 2018. Role of microbial cell properties on bacterial pathogen and coliphage removal in biochar-modified stormwater biofilters. Environ. Sci.: Water Res. Technol. 4 (12), 2160–2169. https://doi.org/10.1039/c8ew00297e.

Andreoli, F.C., Sabogal-Paz, L.P, 2020. Household slow sand filter to treat groundwater with microbiological risks in rural communities. Water Res. 186, 116352 https://doi.org/10.1016/j.watres.2020.116352.

Bai, X., Dinkla, I.J.T., Muyzer, G., 2022. Microbial ecology of biofiltration used for producing safe drinking water. Appl. Microbiol. Biotechnol. 106 (13–16), 4813–4829. https://doi.org/10.1007/s00253-022-12013-x.

Bertelkamp, C., Verliefde, A.R.D., Reynisson, J., Singhal, N., Cabo, A.J., de Jonge, M., Van der Hoek, J.P, 2016. A predictive multi-linear regression model for organic micropollutants, based on a laboratory-scale column study simulating the river bank filtration process. J. Hazard. Mater. 304, 502–511. https://doi.org/10.1016/j.jhazmat.2015.11.003.

Bicudo, B., van Halem, D., Trikannad, S.A., Ferrero, G., Medema, G., 2021. Low voltage iron electrocoagulation as a tertiary treatment of municipal wastewater: removal of enteric pathogen indicators and antibiotic-resistant bacteria. Water Res. 188, 116500.

Boe-Hansen, R., Albrechtsen, H.J., Arvin, E., Jørgensen, C., 2002. Dynamics of biofilm formation in a model drinking water distribution system. J. Water Supp.: Res. Technol. - AQUA 51 (7), 399–406. https://doi.org/10.2166/aqua.2002.0036.

Bradford, S.A., Simunek, J., Bettahar, M., Van Genuchten, M.T., Yates, S.R., 2003. Modeling colloid attachment, straining, and exclusion in saturated porous media. Environ. Sci. Technol. 37 (10), 2242–2250. https://doi.org/10.1021/es025899u.

British Standards Institution, 1990b. Determination by Mass-Loss on ignition. British standard Methods of Test for Soils for Civil Engineering Purposes. Chemical and Electro-Chemical Tests. BS 1377:3:1990:4. BSI, London.

Chan, S., Pullerits, K., Riechelmann, J., Persson, K.M., Rådström, P., Paul, C.J., 2018. Monitoring biofilm function in new and matured full-scale slow sand filters using flow cytometric histogram image comparison (CHIC). Water Res. 138, 27–36. https://doi.org/10.1016/j.watres.2018.03.032.

Chen, L., Zhai, Y., van der Mark, E., Liu, G., van der Meer, W., Medema, G., 2021. Microbial community assembly and metabolic function in top layers of slow sand

filters for drinking water production. J. Clean. Prod. 126342 https://doi.org/10.1016/j.jclepro.2021.126342.
Chrysikopoulos, C.V., Aravantinou, A.F., 2012. Virus inactivation in the presence of quartz sand under static and dynamic batch conditions at different temperatures. J. Hazard. Mater. 233–234, 148–157. https://doi.org/10.1016/j.jhazmat.2012.07.002.
de Oliveira, F.F., Schneider, R.P., 2019. Slow sand filtration for biofouling reduction in seawater desalination by reverse osmosis. Water Res. 155, 474–486.
Dizer, H., Grützmacher, G., Bartel, H., Wiese, H.B., Szewzyk, R., López-Pila, J.M., 2004. Contribution of the colmation layer to the elimination of coliphages by slow sand filtration. Water Sci. Technol. 50 (2), 211–214. https://doi.org/10.2166/wst.2004.0127.
Eisfeld, C., Schijven, J.F., van der Wolf, J.M., Medema, G., Kruisdijk, E., van Breukelen, B.M., 2022. Removal of bacterial plant pathogens in columns filled with quartz and natural sediments under anoxic and oxygenated conditions. Water Res. 220 (February), 118724 https://doi.org/10.1016/j.watres.2022.118724.
Elliott, M.A., DiGiano, F.A., Sobsey, M.D., 2011. Virus attenuation by microbial mechanisms during the idle time of a household slow sand filter. Water Res. 45 (14), 4092–4102. https://doi.org/10.1016/j.watres.2011.05.008.
Elliott, M.A., Stauber, C.E., Koksal, F., DiGiano, F.A., Sobsey, M.D., 2008. Reductions of E. coli, echovirus type 12 and bacteriophages in an intermittently operated household-scale slow sand filter. Water Res. 42 (10–11), 2662–2670.
Foppen, J.W.A., Mporokoso, A., Schijven, J.F., 2005. Determining straining of Escherichia coli from breakthrough curves. J. Contam. Hydrol. 76 (3–4), 191–210. https://doi.org/10.1016/j.jconhyd.2004.08.005.
Foppen, J.W., van Herwerden, M., Schijven, J., 2007. Transport of Escherichia coli in saturated porous media: dual mode deposition and intra- population heterogeneity. Water Res. 41 (8), 1743–1753. https://doi.org/10.1016/j.watres.2006.12.041.
Fu, J., Gao, B., Xu, H., Hao, S., Ren, J., Wu, J., Sun, Y., 2023. Effects of biofilms on the retention and transport of PFOA in saturated porous media. J. Hazard. Mater. 443 (PB), 130392 https://doi.org/10.1016/j.jhazmat.2022.130392.
Guo, J.S., Zhang, P., Chen, Y.P., Shen, Y., Hu, X., Yan, P., Yang, J.X., Fang, F., Li, C., Gao, X., Wang, G.X., 2015. Microbial attachment and adsorption-desorption kinetic of tightly bound extracellular polymeric substances on model organic surfaces. Chem. Eng. J. 279, 516–521. https://doi.org/10.1016/j.cej.2015.05.016.
Haig, S.J., Collins, G., Davies, R.L., Dorea, C.C., Quince, C., 2011. Biological aspects of slow sand filtration: past, present and future. Water Sci. Technol.: Water Suppl. 11 (4), 468–472. https://doi.org/10.2166/ws.2011.076.
Haig, S.J., Quince, C., Davies, R.L., Dorea, C.C., Collins, G., 2014. Replicating the microbial community and water quality performance of full-scale slow sand filters in laboratory-scale filters. Water Res. 61, 141–151.
Haig, S.J., Quince, C., Davies, R.L., Dorea, C.C., Collins, G., 2015. The relationship between microbial community evenness and function in slow sand filters. MBio 6 (5). https://doi.org/10.1128/mBio.00729-15.
He, L., Rong, H., Wu, D., Li, M., Wang, C., Tong, M., 2020. Influence of biofilm on the transport and deposition behaviors of nano- and micro-plastic particles in quartz sand. Water Res. 178, 115808 https://doi.org/10.1016/j.watres.2020.115808.
Hijnen, W.A.M., Dullemont, Y.J., Schijven, J.F., Hanzens-Brouwer, A.J., Rosielle, M., Medema, G., 2007. Removal and fate of Cryptosporidium parvum, Clostridium perfringens and small-sized centric diatoms (Stephanodiscus hantzschii) in slow sand filters. Water Res. 41 (10), 2151–2162. https://doi.org/10.1016/j.watres.2007.01.056.
Hijnen, W.A.M., Schijven, J.F., Bonné, P., Visser, A., Medema, G.J., 2004. Elimination of viruses, bacteria and protozoan oocysts by slow sand filtration. Water Sci. Technol. 50 (1), 147–154. https://doi.org/10.2166/wst.2004.0044.
Huisman, L., Wood, W.E., 1974. Slow Sand Filtration. WORLD HEALTH ORGANIZATION.
Jenkins, M.W., Tiwari, S.K., Darby, J., 2011. Bacterial, viral and turbidity removal by intermittent slow sand filtration for household use in developing countries: experimental investigation and modeling. Water Res. https://doi.org/10.1016/j.watres.2011.09.022.
Kianfar, B., Tian, J., Rozemeijer, J., van der Zaan, B., Bogaard, T.A., Foppen, J.W., 2022. Transport characteristics of DNA-tagged silica colloids as a colloidal tracer in saturated sand columns; role of solution chemistry, flow velocity, and sand grain size. J. Contam. Hydrol. 246 (December 2021), 103954 https://doi.org/10.1016/j.jconhyd.2022.103954.
Li, Q., Yu, S., Li, L., Liu, G., Gu, Z., Liu, M., Ren, L., 2017. Microbial communities shaped by treatment processes in a drinking water treatment plant and their contribution and threat to drinking water safety. Front. Microbiol. 8, 2465. https://doi.org/10.3389/fmicb.2017.02465.
Lee, C.O., Boe-Hansen, R., Musovic, S., Smets, B., Albrechtsen, H.J., Binning, P., 2014. Effects of dynamic operating conditions on nitrification in biological rapid sand filters for drinking water treatment. Water Res. 64 (m), 226–236. https://doi.org/10.1016/j.watres.2014.07.001.
Maurya, A., Singh, M.K., Kumar, S., 2020. Biofiltration technique for removal of waterborne pathogens. Waterborne Pathogens. Butterworth-Heinemann, pp. 123–141.
Napotnik, J.A., Baker, D., Jellison, K.L., 2020. Influence of sand depth and pause period on microbial removal in traditional and modified biosand filters. Water Res, 116577.
Oh, S., Hammes, F., Liu, W.T., 2018. Metagenomic characterization of biofilter microbial communities in a full-scale drinking water treatment plant. Water Res. 128, 278–285. https://doi.org/10.1016/j.watres.2017.10.054.
Oudega, T.J., Lindner, G., Derx, J., Farnleitner, A.H., Sommer, R., Blaschke, A.P., Stevenson, M.E., 2021. Upscaling transport of bacillus subtilis endospores and coliphage phiX174 in heterogeneous porous media from the column to the field scale. Environ. Sci. Technol. 55 (16), 11060–11069. https://doi.org/10.1021/acs.est.1c01892.
Pfannes, K.R., Langenbach, K.M.W., Pilloni, G., Stührmann, T., Euringer, K., Lueders, T., Neu, T.R., Müller, J.A., Kästner, M., Meckenstock, R.U., 2015. Selective elimination of bacterial faecal indicators in the Schmutzdecke of slow sand filtration columns. Appl. Microbiol. Biotechnol. 99 (23), 10323–10332. https://doi.org/10.1007/s00253-015-6882-9.
Rodgers, M., Mulqueen, J., Healy, M.G., 2004. Surface clogging in an intermittent stratified sand filter. Soil Sci. Soc. Am. J. https://doi.org/10.2136/sssaj2004.1827.
Schijven, J.F., Van den Berg, H.H.J.L., Colin, M., Dullemont, Y., Hijnen, W.A.M., Magic-Knezev, A., Oorthuizen, W.A., Wubbels, G., 2013. A mathematical model for removal of human pathogenic viruses and bacteria by slow sand filtration under variable operational conditions. Water Res. 47 (7), 2592–2602. https://doi.org/10.1016/j.watres.2013.02.027.
Soliman, M.Y.M., Medema, G., Bonilla, B.E., Brouns, S.J.J., van Halem, D., 2020a. Inactivation of RNA and DNA viruses in water by copper and silver ions and their synergistic effect. Water Res. X (9), 100077. https://doi.org/10.1016/j.wroa.2020.100077.
Soliman, M.Y.M., van Halem, D., Medema, G., 2020b. Virus removal by ceramic pot filter disks: effect of biofilm growth and surface cleaning. Int. J. Hyg. Environ. Health 224 (December 2019). https://doi.org/10.1016/j.ijheh.2019.113438.
Sousi, M., Liu, G., Salinas-Rodriguez, S.G., Chen, L., Dusseldorp, J., Wessels, P., van der Meer, W., 2020. Multi-parametric assessment of biological stability of drinking water produced from groundwater: reverse osmosis vs. conventional treatment. Water Res. 186, 116317.
Stott, R., May, E., Matsushita, E., Warren, A., 2001. Protozoan predation as a mechanism for the removal of cryptosporidium oocysts from wastewaters in constructed wetlands. Water Sci. Technol. 44, 191–198. https://doi.org/10.2166/wst.2001.0828.
Tatari, K., Smets, B.F., Albrechtsen, H.J., 2016. Depth investigation of rapid sand filters for drinking water production reveals strong stratification in nitrification biokinetic behavior. Water Res. 101, 402–410. https://doi.org/10.1016/j.watres.2016.04.073.
Tripathi, S., Champagne, D., Tufenkji, N., 2011. Transport Behavior of Selected Nanoparticles with different Surface Coatings in Granular Porous Media coated with Pseudomonas aeruginosa Biofilm. Environ. Sci. Technol. 46 (13), 6942–6949. https://doi.org/10.1021/ES202833K.
Unger, M., Collins, M.R., 2008. Assessing Escherichia coli removal in the *Schmutzdecke* of slow-rate biofilters. J. Am. Water Work. Assoc. 100 (12), 60–73.
van der Kooij, D., Veenendaal, H.R., van der Mark, E.J., Dignum, M., 2017. Assessment of the microbial growth potential of slow sand filtrate with the biomass production potential test in comparison with the assimilable organic carbon method. Water Res. 125, 270–279. https://doi.org/10.1016/j.watres.2017.06.086.
Wakelin, S., Page, D., Dillon, P., Pavelic, P., Abell, G.C.J., Gregg, A.L., Anderson, G., 2011. Microbial community structure of a slow sand filter schmutzdecke: a phylogenetic snapshot based on rRNA sequence analysis. Water Sci. Technol.: Water Suppl. 11 (4), 426–436. https://doi.org/10.2166/ws.2011.063.
Weber-Shirk, M.L., Dick, R.I., 1997a. Biological mechanisms in slow sand filters. J. Am. Water Work. Assoc. 89 (1), 87–100. https://doi.org/10.1002/j.1551-8833.1997.tb08164.x.
Weber-Shirk, M.L., Dick, R.I., 1997b. Physical-chemical mechanisms in slow sand filters. J. Am. Water Work. Assoc. 89 (1), 87–100. https://doi.org/10.1002/j.1551-8833.1997.tb08164.x.
Xiao, Y., Wiesner, M.R., 2013. Transport and retention of selected engineered nanoparticles by porous media in the presence of a biofilm. Environ. Sci. Technol. 47 (5), 2246–2253. https://doi.org/10.1021/es304501n.